A DC Voltage Dependent Switchable Acoustically Coupled BAW Filter Based on BST-on-Silicon Composite Structure

Seyit Ahmet Sis, Victor Lee, Jamie D. Phillips and Amir Mortazawi

Department of Electrical Engineering and Computer Science, University of Michigan,
Ann Arbor, MI 48109, USA

***Abstract* — A DC voltage dependent switchable, bulk acoustic wave (BAW) filter is presented in this paper. The filter has a composite structure consisting of a barium strontium titanate (BST) layer sandwiched between top and bottom platinum (Pt) electrodes deposited on silicon (Si) and oxide (SiO_2) layers. The electrostrictive property of ferroelectric BST allows for the filter to be turned on and off by applying an electric field across the BST layer. The Si and SiO_2 layers are used to increase the overall quality factor and mechanical strength of the structure. When the filter is turned on, the 3 dB bandwidth is 43 MHz at a center frequency of 1.08 GHz. After resonating out the input and output static capacitances of the filter using shunt inductors, the filter exhibits an insertion loss of 8.5 dB with the application of 25 V DC bias. The return loss and out-of-band rejection of the filter are 18 dB and 29 dB, respectively. In its off state, with no DC bias applied, the isolation between input and output ports is 37 dB.**

***Index Terms* — Barium strontium titanate, ferroelectric devices, acoustically coupled filters, intrinsically switchable devices, radio-frequency (RF) microelectromechanical systems (RF-MEMS)**

I. Introduction

BAW resonators and filters, as frequency selective elements, are one of the main components of today's modern radios. Thin film bulk acoustic wave resonator (FBAR) filters are commercially available and have been used at the front-end of receiver and transmitter circuits [1]. FBAR filters employ two or more resonators in a ladder form configuration as shown in Fig.1(a). At frequencies away from the resonance frequency (out-of-band), each FBAR resonator behaves as a capacitor. Therefore an FBAR filter can be modeled with a capacitive network as shown in Fig.1(b). At out-of-band frequencies, there is an electrical feed through between the input and output ports via the static capacitances of FBAR resonators. Hence a low out of band rejection is expected for a filter with small number of resonators. However, increasing the number of resonators leads to drawbacks such as higher insertion loss in the pass-band and a larger footprint.

Acoustically coupled filters, on the other hand, can provide higher isolation between the input and output ports. Due to this isolation, an improved out-of-band rejection can be obtained with the same number of resonators as FBAR filters. In acoustically coupled filters, there is no electrical connection between the resonators except from very small feed thru capacitance between the top electrodes. Fig. 1(c) and Fig. 1(d) show the schematic for an acoustically coupled filter with two resonators near the resonance frequency (ω_r) and away from ω_r, respectively. C_f represents the feed thru capacitance and its value is much smaller than the static capacitance of the resonators.

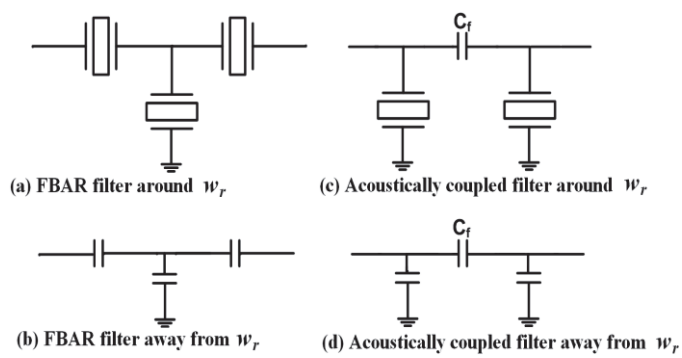

Fig. 1. Schematics of ladder type FBAR filter (a)-(b) and acoustically coupled filter (c)-(d).

The acoustically coupled filter mentioned above is very similar to monolithic crystal filters (MCF) [2]-[4]. Traditional MCF filters were fabricated by using thick quartz crystal plates. In recent years, thin film piezoelectric materials like aluminum nitride (AlN) and zinc oxide (ZnO) have been utilized in the design of acoustically coupled filters [5]-[6]. However AlN and ZnO based filters require external switches for the design of filter banks. RF switches increase the chip area, power consumption, losses as well as the circuit complexity.

In this work, we report on the design of an acoustically coupled filter fabricated by using thin film BST. The property which makes BST the preferred material for this application is its DC voltage induced piezoelectricity or electrostriction, which allows the filter to be turned on and off by applying a DC bias voltage to the top and bottom electrodes.

In this design, top electrodes have an interdigitated structure to increase the transduction and suppress the spurious response hence reducing the filter's insertion loss [5]. The filter is a multilayer composite structure and consists of a sandwiched BST layer on top of Si and SiO_2 layers. The cross-section schematic of an interdigitated acoustically coupled filter is shown in Fig. 2.

978-1-4673-1088-8/12/$31.00 ©2012 IEEE

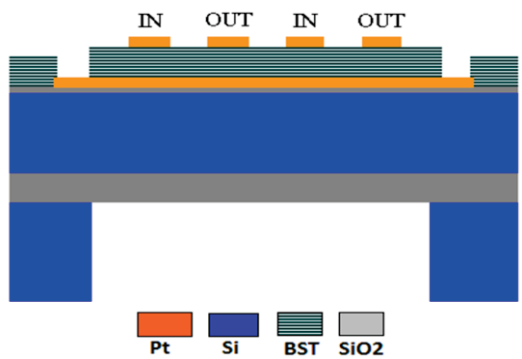

Fig. 2. Cross-section schematic of an interdigitated acoustically coupled filter.

II. Fabrication

The fabrication process for the acoustically coupled filters starts with a silicon-on-insulator (SOI) wafer which has a total thickness of 400 um. The SOI wafer has 2.5 µm layer of high resistivity device silicon and a 2 um layer of buried oxide. A 100 nm layer of thermal oxide is grown on top of the device layer. A 100 nm layer of platinum bottom electrode is deposited and patterned by e-beam evaporation and lift-off. A 1200 nm BST layer is then deposited by pulsed laser deposition (PLD) using an excimer laser and a substrate temperature of 650 °C in a 300 mT oxygen environment. A 100 nm layer of platinum top electrode is deposited and patterned by e-beam evaporation and lift-off. The BST thin film is then selectively etched using diluted HF to reach the bottom electrode of the device. A 500 nm layer of gold is then deposited to serve as the probe contact pads. Finally, the thick silicon handling layer underneath of the device is etched by deep reactive ion etching (DRIE).

III. Measurement Results

The acoustically coupled filters were measured with 150 µm pitch size GSG probes. S-parameters were acquired by using an Agilent E8364B vector network analyzer. The measurement set up is calibrated with short-open-load-thru (SOLT) calibration. Devices are biased through bias tees at the input and output ports. A microscope photo of the measured device is shown in Fig. 3. The device shows an insertion loss and a return loss of 11 dB and 6 dB, respectively. A 6.8 nH shunt inductor is connected at both input and output ports to resonate out the static capacitance of each resonator. The static capacitance of each resonator was determined by modeling the filter with the equivalent circuit shown in Fig. 5. The value of this capacitance is also verified with the calculations based on the extracted dielectric constants of the film at different bias voltages. The filter shows an insertion loss of 8.5 dB and a return loss of 18 dB after resonating out the static capacitance. The system impedance for the measurement results is 50 Ω.

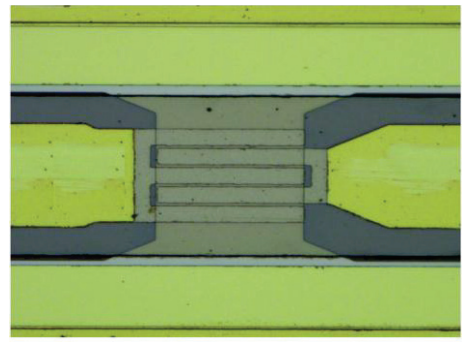

Fig. 3. Microscope photo of the measured device.

The insertion loss and return loss of the device, before and after the inductive tuning, with 25 V dc bias voltage applied, are plotted in Fig. 4. The insertion loss includes the parasitics due to measurement pads that have not been de-embedded.

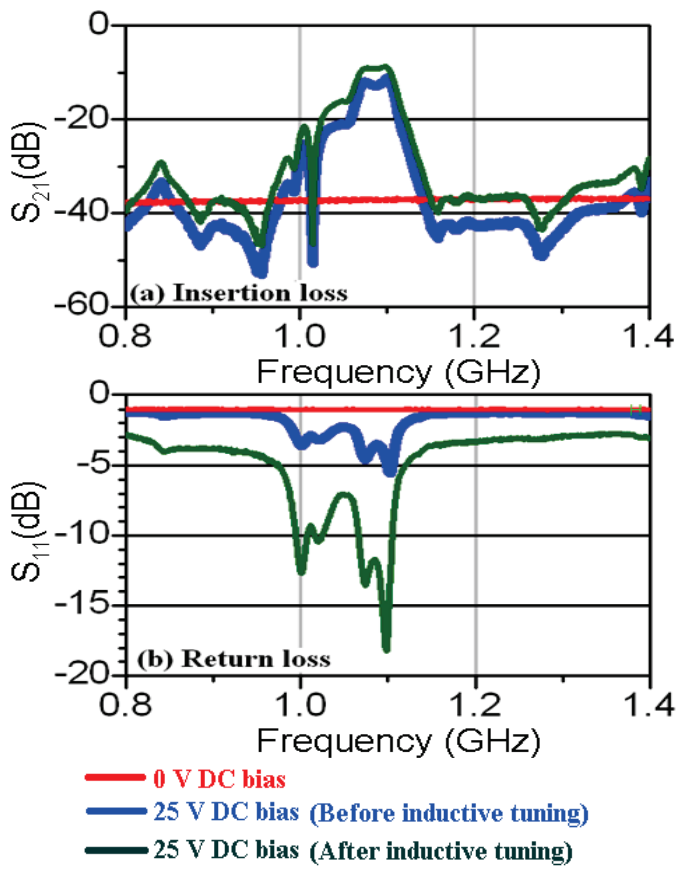

Fig. 4. Insertion loss (a) and the return loss (b) of the measured filter.

Fig. 4 shows spurious resonances below the pass band frequency of the filter. These spurious resonances degrade the filter response and it is believed that these are undesired lateral or plate waves that are also common in FBAR resonators [7].

978-1-4673-1088-8/12/$31.00 ©2012 IEEE

IV. Filter Modeling and Analysis

The device is modeled using the equivalent circuit shown in Fig. 5 [6]. Each component of the model corresponds to the physical properties of the device and the values of each components are tabulated in Table I. The comparison of the lumped element model and the measurement result is shown in Fig. 6.

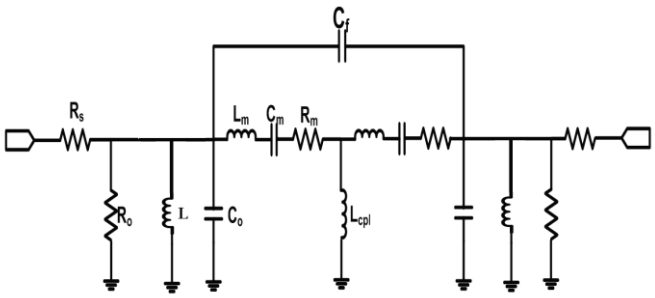

Fig. 5. Equivalent circuit model of the acoustically coupled filter.

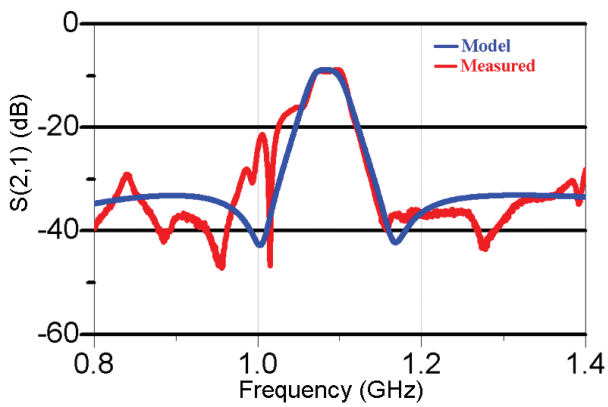

Fig. 6. Comparison of equivalent circuit model and measurement results of acoustically coupled filter.

TABLE I
MODEL PARAMETER VALUES OF THE EQUIVALENT CIRCUIT

R_S (Ω)	4	Conductor loss
C_O (pF)	3.2	Static capacitance
R_O (Ω)	700	Dielectric loss and leakage
L_m (nH)	525	Material density, viscosity and geometry dependent
C_m (fF)	40	Material elasticity and geometry dependent
R_m (Ω)	70	Mechanical loss and electromechanical coupling
C_f (fF)	65	Feed thru capacitance between resonators
L_{cpl} (nH)	15	Acoustic coupling between resonators
L (nH)	6.8	Static capacitance tuning inductor

Detailed analysis shows that, the insertion loss has the largest dependency on R_m in the model. Reducing the value of R_m from 70 Ω to 10 Ω improves the insertion loss from 11 dB to 3 dB. R_m physically represents the acoustic quality factor and is dependent on the acoustic qualities of each layer. C_O is the second most significant parameter affecting the insertion loss. More than 2 dB of insertion loss improvement is obtained when C_O is tuned out with shunt inductor as shown in Fig. 4.

VII. Conclusion

The results of an acoustically coupled filter are presented in this paper. With its small feed-thru capacitance between input and output ports, 29 dB of out-of-band rejection is obtained with only two coupled resonators (2-pole). The filter is turned on and off by controlling the DC bias voltage so that it is not in need of any RF switches on the signal path. A detailed study is on going in acoustically coupled filters to improve the filter with optimum designs.

Acknowledgment

This work is partially funded by the National Science Foundation and ARL MAST program. It is performed at the Lurie Nanofabrication Facility, a member of the National Nanotechnology Infrastructure Network, which is supported in part by the National Science Foundation.

REFERENCES

[1] Ruby, R.; Bradley, P.; Clark, D.; Feld, D.; Jamneala, T.; Kun Wang; , "Acoustic FBAR for filters, duplexers and front end modules," *Microwave Symposium Digest, 2004 IEEE MTT-S International* , vol.2, no., pp. 931- 934 Vol.2, 6-11 June 2004.

[2] Sykes, R.A.; Beaver, W.D.; , "High Frequency Monolithlc Crystal Filters with Posslble Application to Single Frequency and Single Side Band Use," *20th Annual Symposium on Frequency Control. 1966* , vol., no., pp. 288- 308, 1966

[3] Beaver, W.D.; , "Theory and Design of the Monolithic Crystal Filter," *21st Annual Symposium on Frequency Control. 1967* , vol.,no.,pp.179-199,1967

[4] Rennick, R.C.; , "An Equivalent Circuit Approach to the Design and Analysis of Monolithic Crystal Filters," *Sonics and Ultrasonics, IEEE Transactions on* , vol.20, no.4, pp. 347- 353, Oct 1973

[5] Abdolvand, R.; Ayazi, F.; , "Monolithic Thin-Film Piezoelectric-on-Substrate Filters," *Microwave Symposium, 2007. IEEE/MTT-S International* , vol., no., pp.509-512, 3-8 June 2007

[6] Wanling Pan; Abdolvand, R.; Ayazi, F.; , "A low-loss 1.8GHz monolithic thin-film piezoelectric-on-substrate filter," *Micro Electro Mechanical Systems, 2008. MEMS 2008. IEEE 21st International Conference on* , vol., no., pp.176-179, 13-17 Jan. 2008

[7] Bi, F.Z.; Barber, B.P.; , "Bulk acoustic wave RF technology," *Microwave Magazine, IEEE* , vol.9, no.5, pp.65-80, Oct. 2008